BioMechanical Orthotic Knee Joint for Exoskeletons Thesis

Alex Tacescu

Masters Thesis in Robotics Engineering

Robotics Engineering Department

Worcester Polytechnic Institute

May 2021

Contents

List of Figures

List of Tables

Abstract

Chapter 1

Introduction

test

Chapter 2

Background

2.1 Paraplegia and Rehabilitation

Paraplegia is a medical term used to define where a patient loses feeling and/or movement in their lower two limbs. In comparison, quadriplegia (also sometimes known as tetraplegia) is the loss of control in all four limbs. It is important to note that not all feeling/movement needs to be lost in order for someone to be considered paraplegic [5]. Only 30% of all paraplegic and quadriplegic patients are considered complete lesions, where there is no sensation and no mobility in the lower limbs [12].

Paralysis is usually caused by trauma, such as sports injuries, vehicle accidents, or accidental falls, when the spine gets injured (see Figure 2.1). However, it can also be caused by specific diseases, including multiple sclerosis, amyotrophic lateral sclerosis, stroke, and in specific cases cancer [19]. Common effects of
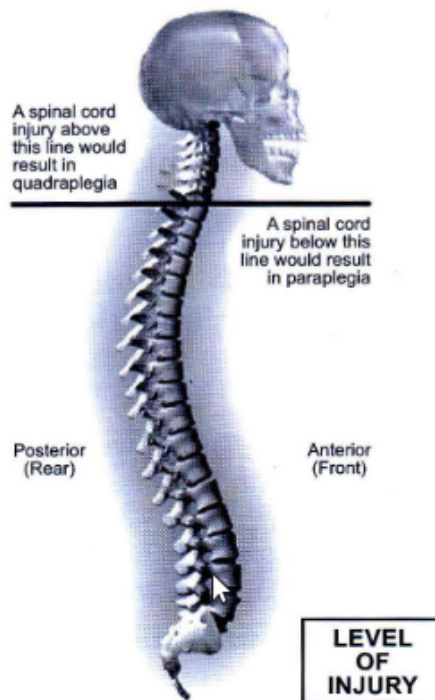
Figure 2.1: Location of spinal chord injury will determine type of paralysis [12]

paraplegia include:

- Loss of mobility, reflexes, and sensation

- Muscular weakness and atrophy

- Hormonal variations

- Gastrointestinal and bowel/bladder problems

- Muscle spasms

- Reduced cardiorespiratory fitness and increased likelihood of cardiorespiratory issues

Rehabilitation can play a key role in reducing these side effects in patients who experience paraplegia. Mainly, physical therapy for paralysis patients focus on three main types of exercises: stretching, strengthening, and aerobic. Additionally, paralysis patients may go through gait training with the assistance of medical devices.

2.1.1 Physical Therapy for Paralysis Patients

Stretching

Stretching is considered one of the most important exercises [12], more-so than any other form of exercise because it can be done often and at home. Carefully designed exercises (like seen in Figure 2.2) can improve flexibility, reduce muscle spasms, reduce the chance of injury, and relieve contractures [18] [9] [20]. Some common stretches include bilateral adductor stretches, quadriceps stretches, and hip flexor stretches.

Cardiorespiratory and Cardiovascular Training

Due to the difficulty of exercise, cardiovascular and cardiorespiratory activities are also very important to maintain health in paralysis patients. Aerobic exercises can increase energy levels, improve lung and heart function, control body weight, and reduce fatigue [12] [6]. A study showed that patients who suffer from neuromuscular deficiencies such as paraplegia suffered decreasing VO_2 max compared
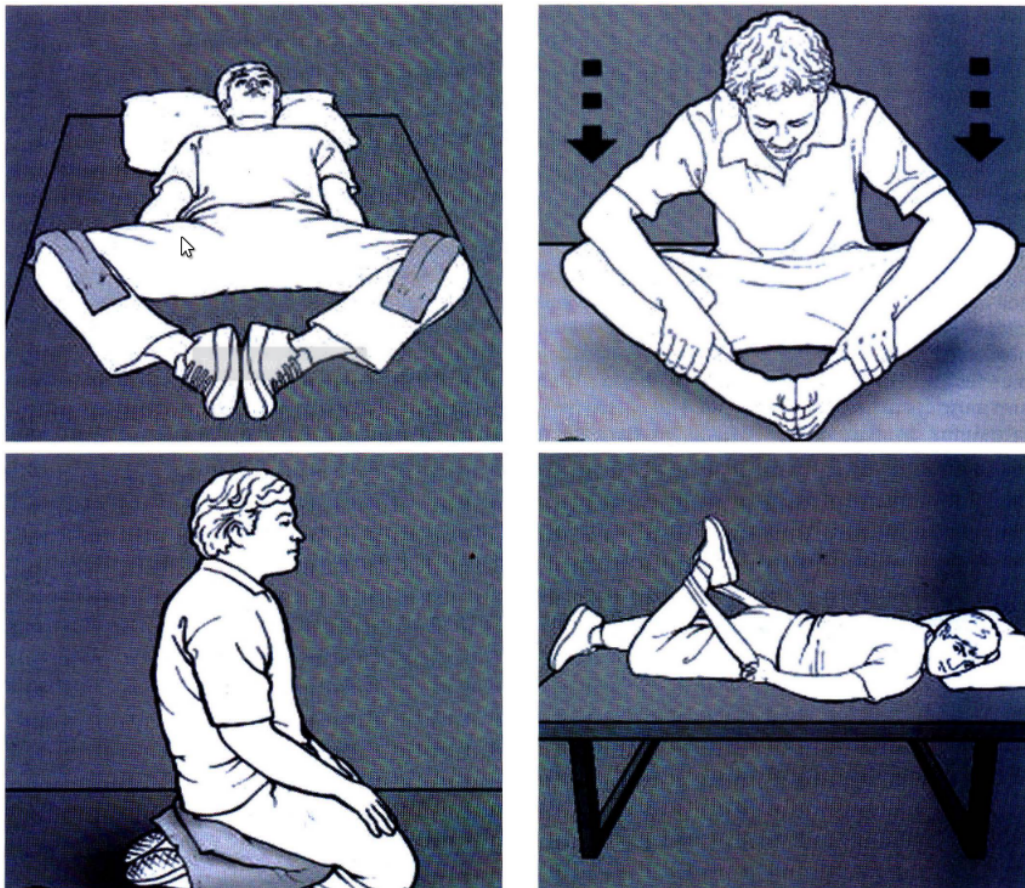
Figure 2.2: Bilateral Adductor Stretches (top) and Quadriceps Stretches (bottom) for paraplegic and quadriplegic patients [12]

to control subjects with no issues [6]. VO_2 max a common metric that measures the maximum rate of oxygen utilization during heavy exercise. Combination of the upper body and lower body in paraplegic patients can strengthen the paralyzed limbs while also activating healthy limbs. Some researchers have even proposed introducing wheelchair racing as a sport in an effort to help with rehabilitation after paraplegia [17].

Strength Training

Improving strength in muscles may actually partially reverse the loss of mobility in partially paralyzed patients, while also improving muscle tone [6] and preventing bone atrophy [18]. This type of exercise can be split into two major regions: training of affected limbs and muscles, and the training of non-affected regions. Affected limbs can benefit from an increase in mobility and definition, and can generally reduce the likelihood of muscular atrophy. Additionally, strong hip and leg muscles in partially paraplegic patients can help in gait training and increase the possibility of usage in life. On the other side, increasing or maintaining strength in unaffected regions can help with quality of life improvement. Often, paraplegic patients may elect to use crutches or canes as an assisted mobility device in the real world. Increasing arm/shoulder strength and endurance will also increase capability for patients to use some of these assisted devices. Finally, back and abdomen muscles are very important to strengthen to maintain posture and improve gait performance [3].

Hydrotherapy

Hydrotherapy (exercising in water) is a notable way for patients suffering from paraplegia to better strengthen muscles and improve cardiovascular health. Due to similar buoyancy, water can reduce the effects of gravity without any external assistive devices. At the same time, the increased density of the water (in comparison to air) creates a natural resistance without the use of weights or elastics.

Therefore, hydrotherapy is used in paraplegic patients to increase muscle power, increase endurance, and even help with gait training (see subsection 2.1.2). In minor cases of paralysis, some patients even use swimming as a way to exercise [12] [22].

2.1.2 Gait Training

Gait training has become the best way to improve motor functions in those who have partially or fully lost mobility in their legs and torso. The premise of this exercise is to have patients do similar movements to what one would do without their disability, like walking and climbing stairs. Essentially, the goal is to help the patient relearn the gaits they previously knew. Spinal neuronal circuits degrade quickly - in just a year, they can lose most of their potency, essentially unlearning any gait abilities the patient had in the past [7] [12] [3]. Gait training can help reconnect the broken spinal neurons, and improve motor function and balance in a patient. In fact, several studies have show that some patients with full spinal chord injuries have been able to recover part or even all of their walking capabilities through gait training [7] [23]! [1]

Use of Assistive Devices for Gait Training

Since most patients suffering from paralysis won't be able to hold themselves up, there have been many different proposals to compensate for gravity. At lower

---

[1]There is significant research in the benefits of gait training for paraplegic and quadriplegic patients. Not all prior work is cited here.

levels of paralysis, canes, walkers, and other walking assisted devices can help. Hydrotherapy has also been used with gait training due to the similar densities of humans and water [22]. With more serious cases of paralysis, robotic solutions and other active orthotics have been proposed and used in clinical settings.

Standard solutions like canes and walkers will only work for patients with mild paralysis. Canes are designed to support only 25% of body weight [12]. They can also be fairly unstable, since they usually only have at most 4 points of contact with a very small ground contact area. Walkers are better than canes, since they can support up to 50% of body weight [12]. However, canes, walkers, and crutches have one downside: the required upper-body strength. Mild lower-limb paralysis cases usually can benefit from these inexpensive tools to help with gait training. However most patients will struggle holding themselves up during gait training.
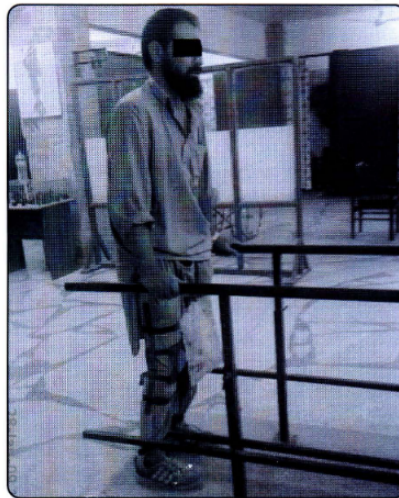
Figure 2.3: Patient using basic splint orthosis [12]

8

Orthosis are the next level up in assistive devices. They can come in many different shapes and can be designed to fit a patient's progress. At the lowest levels are specialty splints or braces (seen in Figure 2.3) that can help keep joints locked or reduce load of a joint through passive springs. These solutions often cost very little in material, and apply normal loads on the user's skeletal system - helping to prevent bone atrophy. Actively powered orthosis also exist with various levels of research and clinical trials (see section 2.3), and can be separated in two major groups.
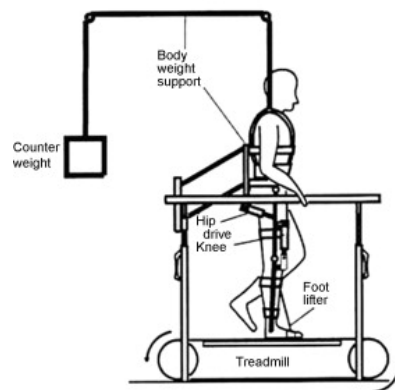
Figure 2.4: Comparison between an exoskeleton with active gravity compensation (left) and an exoskeleton with passive gravity compensation (right) [7]

TODO: Add additional figure of an active GCS exo

Actively compensating exoskeletons (see left image in Figure 2.4) are orthosis devices that use various types of actuators, sensors, and gait controllers to help keep patients standing and walking with little to no strength required (from the patient). These types of exoskeletons use up a significant amount of energy, since they must essentially do all the physical work that leg muscles would normally do.

This usually means very powerful actuators and motors with precise and stable control, and large batteries (which add to overall weight) or a large/long tether. Such power increases the overall flexibility of the system, however, at a cost. It also increases complexity of the control software, and introduces a safety risk of attaching powerful actuators to patient limbs.

To mitigate some of these risks, some solutions separate the exoskeleton and the gravity compensation (see right image in Figure 2.4). A separate mechanical system supports the weight of the user usually through a counterweight system or a gantry of some sort. This allows for the actuator in the exoskeleton orthosis to be weaker or power (current) limited to prevent injury in case of a malfunction. However, such systems are much more limited in their uses, since the power is hardware limited and more infrastructure is needed to use the device. Additionally, any actively compensating exoskeleton orthosis can be current limited and be used with a mechanical gravity compensation system.

However, one of the biggest struggles with orthoses is the dermatological problems that they may cause. As explained earlier, patients suffering from paralysis are at an increased risk of developing skin complications [8]. This can be at least partially attributed to reduced sensitivity in paralyzed areas of the body. Therefore, any assisted devices that attach to a patient's skin should accurately follow the natural trajectory of the skin to avoid unnecessary rubbing.

Robotics for Paralysis Rehabilitation

Robotics have a very large opportunity to improve the rehabilitation process in paraplegic patients. Clinical research in using robotic orthosis for gait training and other rehabilitation exercises show positive improvement in most patients when considering quality of life [11] [2].

> **IMPROVE:**
> Add more to this part

2.2   Human Knee Model

The human knee was initially considered as a pin joint, but research as early as 1992 suggested differently [15]. This study showed that the joint does extend as it bends by attaching motion capture markers to the femur and tibia of 5 different subjects. It also suggested that there was a difference between loaded and unloaded knees.

Several studies since then have confirmed a non-linear knee flexion and extension relationship, as well as the difference between loaded and unloaded knees. Instead of intrusive motion capture markers, modern Magnetic Resonance Imaging (MRI) and advanced motion capture systems [14] has allowed for more precise bone tracking for both unweighted and weighted knee joints, since a 3 dimensional model can be built of the joint. A study performed by Iwaki *et. al* using MRI data of cadaver knee joints found that the femur posterior circular arc is responsible for the linear extension of the leg through the flexion process, similar to the movement of a mechanical cam (see Figure 2.5) [13]. Through the bending process, the joint didn't rotate much outside the plane of flexion. These results
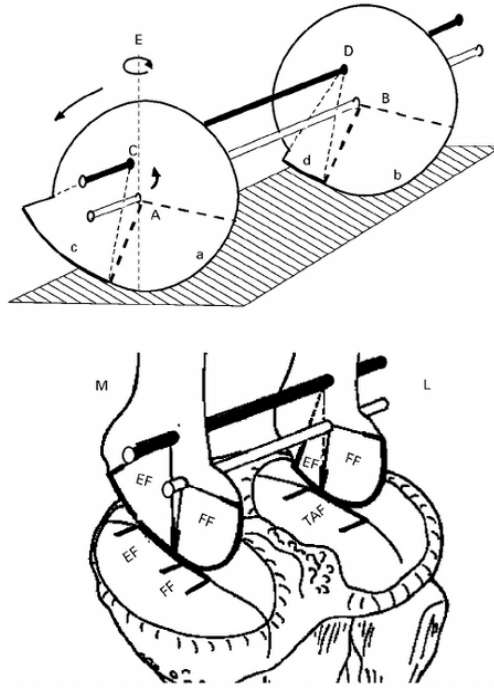
Figure 2.5: Diagram from [13] depicting the internal anatomy of a knee with respect to the movement patterns. The movement characteristics can be closely related to a cam mechanism

were further confirmed during the dissection of the cadavers as well as in the followup research with live human knee joints [10]. Additionally, the research also showed tibiofemoral motion moved forward roughly 4mm when the knee joint was loaded.

This research was taken a step further with the parameterization of a knee joint's flexion and extension. The goal was to define a knee joint model to better create artificial mechanisms for rehabilitation exoskeletons. Based on MRI data of unloaded knees from [13], ellipses were fitted to the ends of the tibia and femur to approximate the relationship between the distance r and flexion angle θ. The
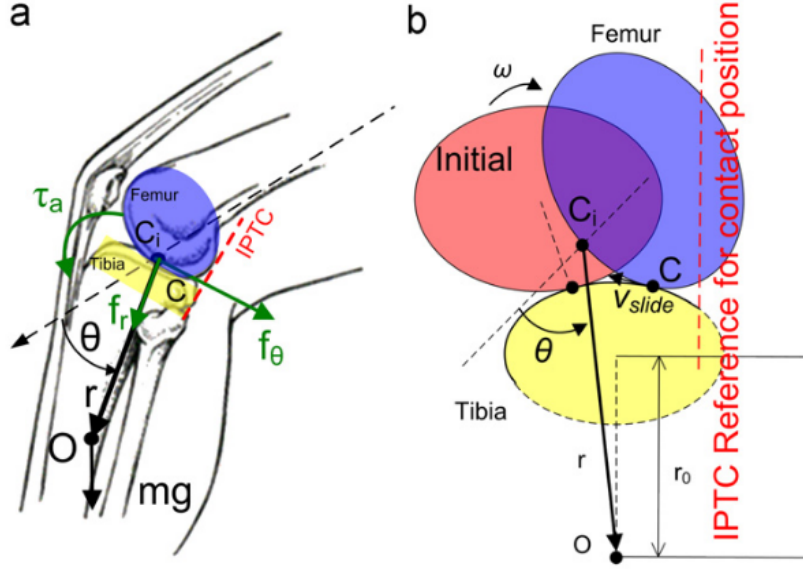
Figure 2.6: Diagram showing knee rotation [16]: (a) demonstrates the tibia's rotation around an initial contact point C_i. (b) shows the femur and tibia relationship using parameterized shapes between the distance r and flexion angle θ

resultant tibia to femur relationship can be seen in Equation 2.1 and Figure 2.7 [16].

$$r(\theta)mm = 1.078\theta^4 - 11.184\theta^3 + 26.524\theta^2 - 0.825\theta + 263.59 \qquad (2.1)$$

These studies measure the relationship of the bones in the knee joints, and not the skin movement around the joint. However, exoskeleton orthosis are usually connected directly to the skin. In order for the research presented above to be applicable to orthosis, a relationship between the skin and femur/tibia must be made. A study by Benoit *et. al* looked at 8 healthy males to compare the bone and
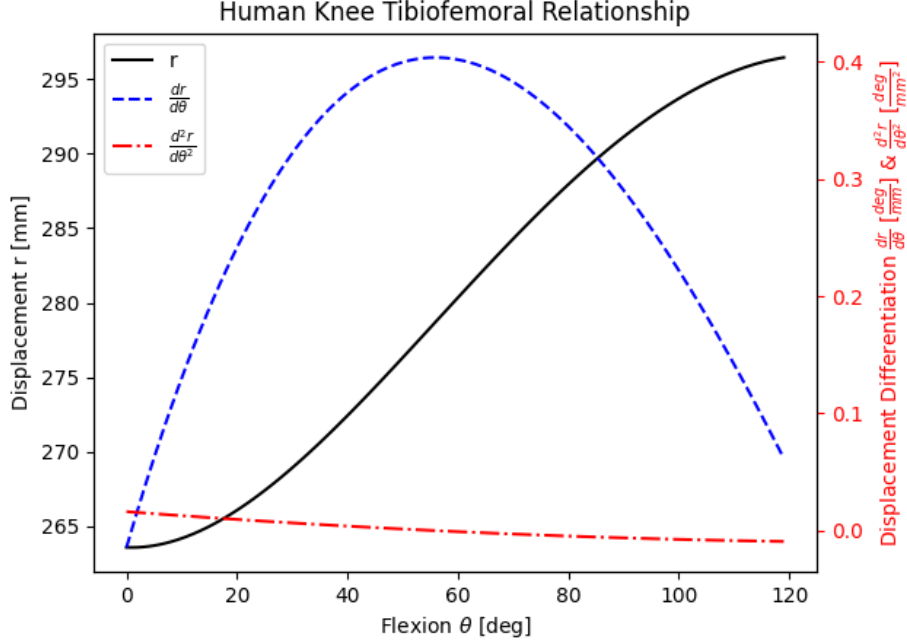
Figure 2.7: Relationship between tibia and femur during the flexion of the joint. $r(m)$ is the distance between joint point of contact (C_i in Figure 2.6) and center of mass of the tibia.

skin movement in and around the knee joint in order to identify if skin markers are sufficient to determine bone kinematics around the knee. Each subject had intra-cortical bone-pins inserted in the proximal tibia and distal femur with 3 motion capture markers on each pin. Then, 8 total motion capture markers were attached directly to the skin to measure the difference in the movement (see Figure 2.8).

The results of this study seemed to show a significant difference between the skin and bone movement during several different gaits; average rotational errors were between $4.4°$ and $13.1°$ while translational errors averaged up to 16.1mm [1]. What is more interesting is that the errors measured remained relatively constant
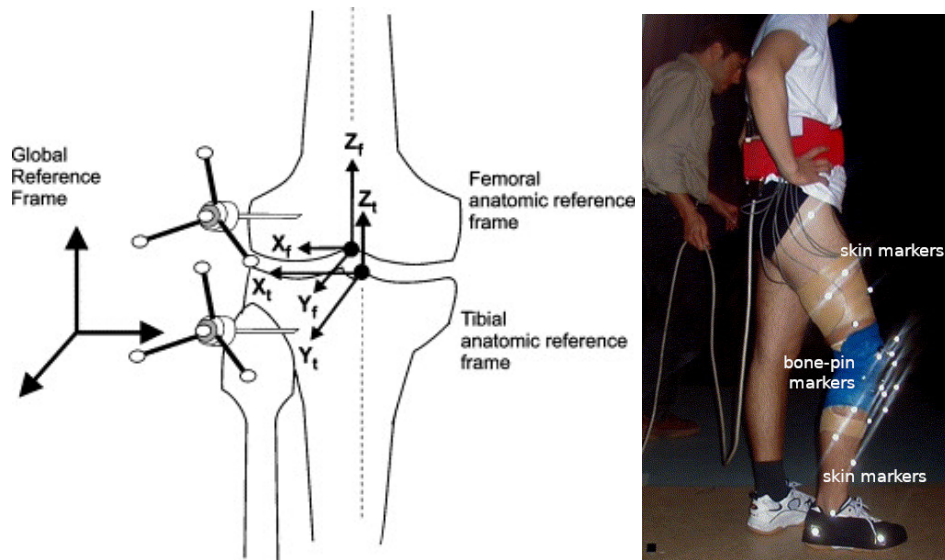
Figure 2.8: Depiction of the research showing the relationship between skin and bone movement: (left) a figure illustrating the location of the bone-pins and (right) showing an image of a subject with all markers attached to them [1]

between different movements, seemingly demonstrating that the error comes from the different connection methods (skin vs bone) and not via measurement tolerances. The researchers were able to conclude that skin-marker kinematics around the knee are not representative of the motion of the bone inside the knee joint. We may be able to therefore inversely conclude that bone kinematics may not be a good representation when designing knee orthoses. However, the research had a relatively small sample size due to the invasive nature of the experiment, and attached markers directly to taped up thighs (see Figure 2.8), which may have failed to represent the actual skin movement. Therefore, more research is needed to conclude the relationship between a skin connection on the thigh and a skin connection on the shank (calf) for the purpose of rehabiliation exoskeletons.

15

2.3 Exoskeleton Orthosis

Exoskeletons are an interesting application to help those with paralysis rehabilitate and exercise their muscles. They can take programmatically reduce or add bodyweight to the user to aid with safe gait training and muscle development. Additionally, powered exoskeletons can help move patient legs in the motion of a gait to help with relearning gait cycles such as walking and climbing stairs. The flexibility these rehabilitation devices offer have been noticed, and several different solutions exist at different levels of clinical implementation.

2.3.1 WPI LARRE
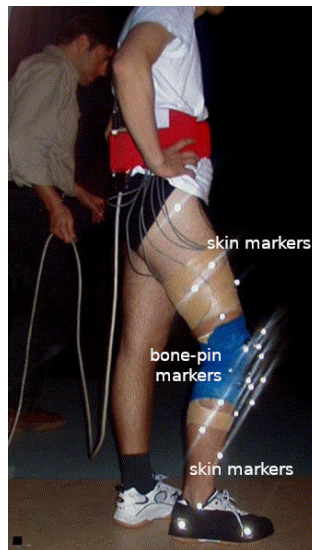
Figure 2.9:

The WPI LARRE (Legged Articulated Robotic Rehabilitation Exoskeleton) is an exoskeleton project developed by the Worcester Polytechnic Institute (WPI)

Automated and Interventional Medicine (AiM) Lab. The research presented in this thesis directly contributes to the AiM Lab's effort to develop an exoskeleton for rehabilitation of lower-limb paralysis patients.

The project was originally started and named as the HEX Gen-1. It's original goal was to help with rehabilitation of patients who have suffered from spinal chord injury, and took a hybrid approach to an exoskeleton design. The hip joint is powered by a brushless DC motor (Maxon EC 90), while the knee and ankle joints aren't actively powered by any motor. Instead, the knee joint contains a spring wrap clutch/brake to help provide support to patients throughout their gait cycles. Additionally, the ankle joint included a spring to add force during dorsiflexion to help in walking gaits [21].

2.3.2   H2

The H2 robotic exoskeleton is designed by the University of Houston to help stroke survivors with gait training and physical rehabilitation. It has 6 powerful DC motors (3 on each leg on the hip, knee, and ankle joint) geared down with harmonic gearboxes. Each motor is powered by its own local motor controller, with all electronics connected to a main controller via CAN bus. An assistive gait controller is used to apply torque when patients deviate from a planned gait pattern. The device itself was tested on 3 hemiparetic stroke patients, and was safe and effective throughout the 4 week testing period. The pilot clinical study demonstrated the "assist-as-needed" control system was able to benefit the stroke patients, and help them recover [4].

Figure 2.10: The H2 Exoskeleton, with 6 powered joints and lithium polymer batteries [4]

2.3.3 ReWalk

2.3.4 EKSO

2.3.5 Indigo

2.3.6 KINESIS

2.3.7 HAL

Chapter 3

Knee Joint Design

3.1 Design Requirements

The following are the design parameters layed out at the beginning of the project:

Follows the defined knee tibiofemoral trajectory

The knee joint must be able to follow a tibiofemoral trajectory. As referenced in [16], human knee joints can be generally defined by a quartic trajectory. This project will use the parameters of a cadaver, which can be seen in Equation 3.1. The design of the joint must be easily customizable for each patient/user. Ideally, all parts except a few should remain the same to increase simplicity and reduce

cost of manufacturing.

$$r(\theta)mm = 1.078\theta^4 - 11.184\theta^3 + 26.524\theta^2 - 0.825\theta + 263.59 \qquad (3.1)$$

Supports the mass of a person

Each joint should be able to support half of the mass of a 85kg human plus a 15kg exoskeleton (total of 100kg) with an additional safety factor.

Power/Torqe/Speed for walking gaits and sit/stand exercises
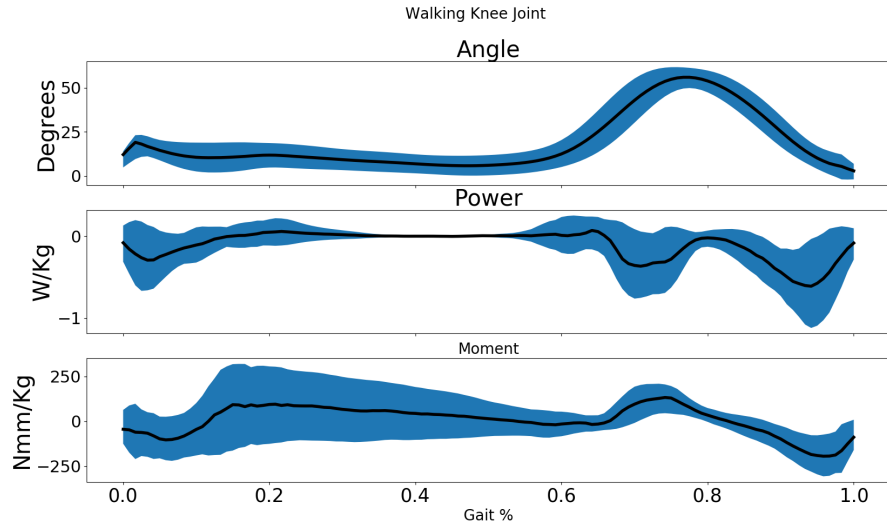
Figure 3.1: Joint kinematics and dynamics during a walking gait cycle [21]

The knee joint has two rehabilitation requirements to fulfill: walking gaits and sit/stand gaits. Prior research has shown that walking gaits require roughly up to
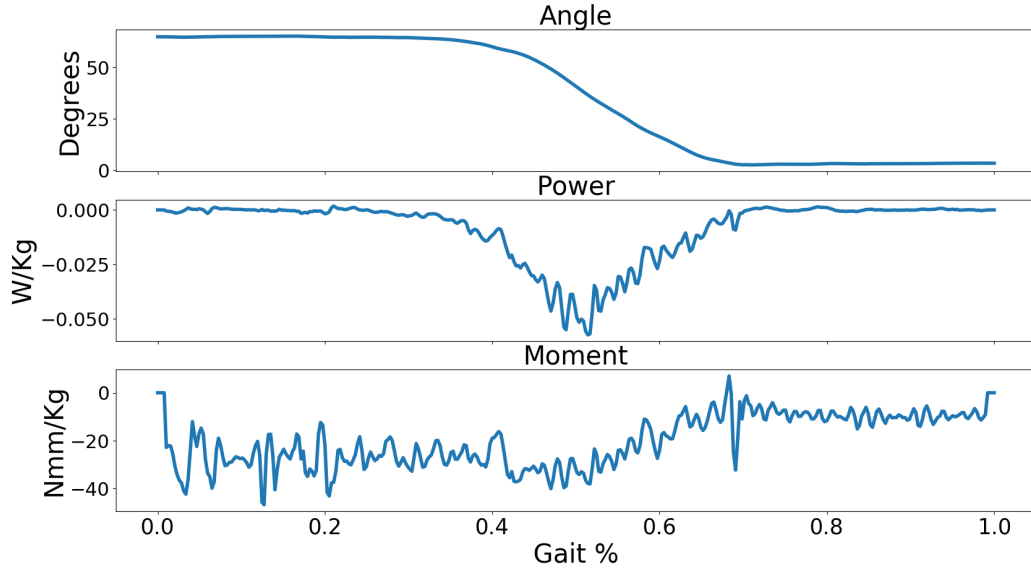
Figure 3.2: Joint kinematics and dynamics during a sit/stand gait cycle [21]

$0.65\frac{W}{kg}$ and $0.25\frac{Nm}{kg}$, (see Figure 3.1), while a sit/stand gait requires roughly up to $0.5\frac{W}{kg}$ and $0.04\frac{Nm}{kg}$. Speed requirements are roughly $12°/sec$ for walking gaits and $15°/sec$ for sit/stand gaits. Therefore, the designed knee joint for the $100kg$ weight specification should be capable of mechanically outputting $65W$ and $25Nm$ at $15°/sec$.

Senses the joint angle

Sensors must be able to accurately encode the rotational position of the joint. The rationale behind this requirement is for research, debugging, and most importantly accurate and safe position control. Therefore, the joint must be able to read its own position in both passive (non-powered) modes and active (powered)

modes. It should also have a minimum accuracy of $\pm 0.5°$ during position control, and be able to maintain position measurement through power cycles (absolute positioning).

Simple to manufacture and assemble

The joint must be designed with manufacturing and assembly in mind. All components must be easily sourced and generally available. Any machining requirement must be achievable with common machining techniques.

IMPROVE: This parameter might need to be more measurable?

Integrates into the WPI LARRE

This research supports the advancement of the WPI LARRE project introduced in subsection 2.3.1. Therefore, the designed joint must be able to integrate into the universal exoskeleton joint connector developed in the LARRE project.

3.2 Mechanical Design

The orthotic joint design proposed uses a similar idea to how a human knee joint works; a cam mechanism extends the shank link as it is rotated relative to the thigh link. The joint therefore has two degrees of freedom: rotation around the center of rotation (output shaft of the motor and gearbox) and translation in the direction of the shank. However, since there is only one actuator, the joint is underactuated; this underactuation can be taken advantage of to match a patient's knee trajectory, where the center of mass of the shank extends away from the joint

center as the joint bends. For ease of assembly, the entire joint is held together by 4 M5 shoulder bolts, which also act as the axles for a total of 10 bearings.

Knee Joint Exploded View
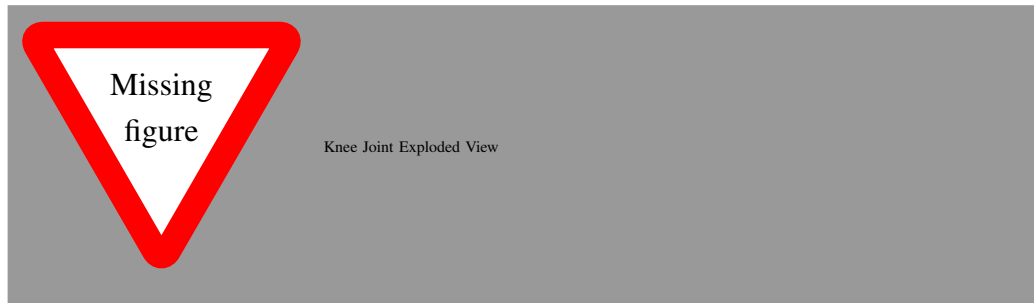
Figure 3.3: Exploded view of the knee joint, with all relevant components labeled

Torsion Bars

The center of rotation of the joint is designed to match the axis of rotation of the actuator. The output of this actuator is directly connected to the torsion bar using M5 shoulder bolts. Each bolt is designed to support 3 bearings: 2 on the motor side and 1 on the patient side. The reduced count on the patient side allows for the torsion bar to be partially recessed in the shank link to reduce the distance between the center of mass between the patient and the joint. The 6 bearings are still able to support the forces necessary throughout a walking gait cycle (see section 3.2).

FIX: Add reference to actuator decision section

Shank Links

The 2 shank links attach to the lower part of the exoskeleton, and are responsible for taking the rotational energy created by the motor and partially changing it

to translational energy to help linearly extend the shank. The bearings connected to the torsion bars ride in a guide built into the shank link. This guide is slightly larger than the bearing diameter (0.3*mm*) to prevent rubbing without creating much of a backlash (0.39° backlash, see calculation on Equation 3.2).

$$Backlash = atan(\frac{\frac{0.3mm}{2}}{22mm}) = 0.39° \qquad (3.2)$$

The surface of the guide must be smooth and parallel to the axis of the bearings to avoid damaging them. Depending on the material and manufacturing method chosen, the surface may require additional machining to ensure it can match these requirements. The length of the guide must be larger than the distance between the centers of the two shoulder bolts plus the maximum distance of linear extension by the knee (Equation 3.3). For this prototype, this length was 78*mm*.

$$GuideLength \geq TorsionBarC2C + MaxKneeExtension = 44mm + 34mm = 78mm$$

$$(3.3)$$

The shank link is also responsible to connect to the lower part of the exoskeleton. Just like the thigh link, this is done through the universal exoskeleton connector developed throughout the WPI LARRE project [21].

The connection between the thigh link and the shank link is very important, as it adds torsional stability and overall rigidness to the entire joint. It was therefore imperative during the design process to create wide surface contact between the thigh and shank links. To reduce the energy lost to friction between these plates,

Missing figure

Add cross section of the joint
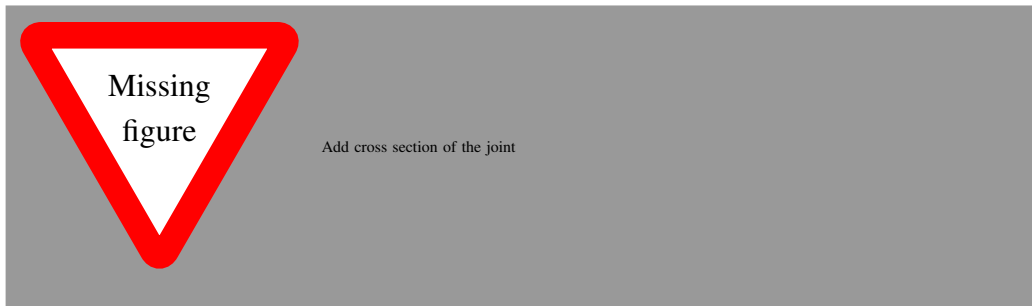
Figure 3.4: A cross section of the knee joint in a $0°$ position

3.2mm thick Delrin® slides were laser cut and attached to the shank link.

Similarly to the torsion bar, the shank link also uses 2 shoulder bolts to clamp the two shank links on the thigh link as well as to give the bearings that ride on the knee path guide a precise surface to mount to. To maintain a consistent clamping force, lock nuts are used since they do not easily back out with movement and vibration.

Thigh Link

The thigh link acts as the main mounting point for most things, as well as contains the knee path guide. Just like the shank link, the thigh link has the universal exoskeleton connector used throughout the WPI LARRE project. The motor bracket is connected to the thigh link at two locations using $20mm\varnothing x50mm$ spacers. These spacers must be strong and stiff, as they transmit the torque between the thigh and shank connector in high load situations. A potentiometer is also mounted inside the thigh link to measure the current angle of the joint, as shown in Figure 3.4. The wire connecting to it is routed through a slot in the thigh link to

avoid any interference with the moving shank links. This wire comes out the top and is connected to the main controller of the exoskeleton.

Knee Path Guide

The knee path guide is built into the thigh link as a slot. The geometry is calculated using several point measurements connected in SolidWorks with a spline. Each point is split by 15 degrees, and calculated from a pre-determined equation. This equation can be measured from a patient knee (see chapter 4), but throughout the design and testing of this knee joint, Equation 3.1 from [16] is used. Figure 3.5 shows the equation above overlayed on the thigh link.

TODO: Verify this number

Missing figure

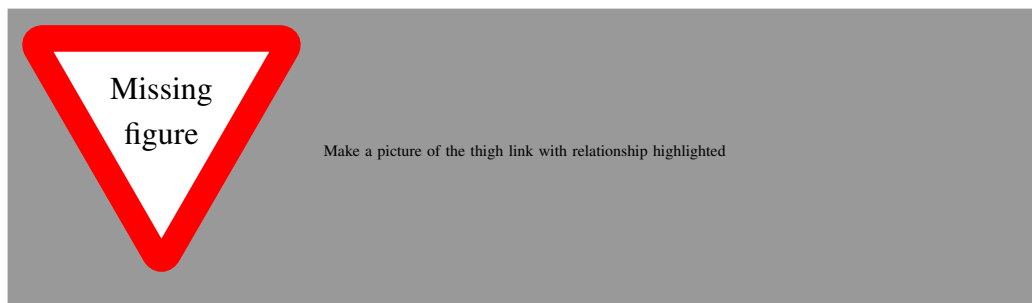Make a picture of the thigh link with relationship highlighted

Figure 3.5: The thigh link contains the geometry which the bearings ride on to mimic the tibiofemoral relationship

The joint is designed to be easily adaptable between patients. Therefore, the only customized part in the entire system is the thigh link which holds the knee path guide. All other parts remain the same to decrease cost and improve repairability.

Input (Motor) Power	P_{input}	$90 Watts$
Input (Motor) Torque @ Nominal	τ_{input}	$0.560 Nm$
Input (Motor) Speed @ Nominal	ω_{input}	$2510 rpm$
Input (Motor) Stall Torque	τ_{in_stall}	$7.480 Nm$
Gearbox Ration	$\frac{n_1}{n_2}$	$100:1$
Output Power	P_{output}	$81 Watts$
Output Torque @ Nominal	τ_{input}	$50.4 Nm$
Output Speed @ Nominal	ω_{input}	$15°/sec$
Output Stall Torque	τ_{out_stall}	$673.2 Nm$

Table 3.1: Motor/gearbox specifications and output power specifications of the proposed joint. See Appendix A for all equations and calculations used.

Torque Requirements & Actuator Selection

The design parameters specified in section 3.1 are an output of at least $65W$ and $25Nm$ at $15°/sec$. The Maxon EC90 was chosen, with a peak power output of $90W$ and a max continuous torque of $0.560Nm$ at $2510rpm$ (see Appendix B). To match the speed and torque requirements, a $100:1$ gearbox ratio is needed. Due to its high reduction to size ratio, a strain wave gearbox from Harmonic Drives™ was chosen.[1] Estimated efficiency of this gearbox is roughly $\varepsilon = 90\%$.

The output power of the joint is $81W$, with a nominal torque of $50.4Nm$ at $15°/sec$. Power, torque, and speed specifications of the joint theoretically exceed the requirements. Physical testing is needed, however, to ensure that these numbers are accurate and sufficient for a rehabilitation exoskeleton.

---

[1]The gearbox used is proprietary, and no datasheet is available

Potentiometer and Rotary Encoder

A potentiometer was embedded into the knee design to act as an absolute rotary encoder to measure the current angle of the joint. It's purpose is twofold: to provide for an absolute angle at any given time and to provide for rough rotary encoding when a the motor (for passive experimentation). As mentioned above, the integration needed to protect the sensitive connection points. The potentiometer chosen was the Vishay PRV6, with 200° of travel, a linear resistance, and $\pm 1\%$ tolerance, which equates to a sensored tolerance of $\pm 2°$.

The motor used also has 3 hall sensors used for pinpointing the position of the rotor versus the stator. Since the motor has a 12 poles and 3 sensors (totaling 36 pulses per revolution) as well as a 100:1 reduction through the gearbox, the hall effect sensors can be used to create an effective 3600 pulses per revolution encoder. When used in conjunction with the absolute encoder, the encoded angle can be very precise.

Bearings

All 10 bearings used in the design are the same (for simplicity and reduction of cost): 19mm outside diameter x 6mm inside diameter x 6mm thick double shielded ball bearings (Model 626ZZ). Each is rated for 2.6kN dynamic load and 1.05kN static load. Before selecting these bearings, two calculations were required to ensure these bearings could support the forces required.

The first is the requirement of the torsion bar. Given the max torque require-

ment for the project is 25Nm and the torsion bar is 44mm from center to center, Equation 3.4 calculates that the total load on all 6 bearings used is 1136N, equaling to roughly 190N per bearing.

$$\text{Total Load per Torsion Bar Bearing}: \frac{1}{6} \times \frac{25Nm}{44mm/2} = \frac{1}{6} \times \frac{25Nm}{0.022m} = 189.4N$$

(3.4)

The second force requirement for these bearings were in the knee path cam. Each knee joint must be able to hold half of the weight requirement of 100kg statically. Equation 3.5 demonstrates that each of the 4 bearings used in the cam will see a maximum static load of 245N per bearing.

$$\text{Total Load per Cam Bearing}: \frac{1}{4} \times 100kg \times 9.81m/s = 245.3N \qquad (3.5)$$

3.3   Material Selection & Manufacturing

Material Analysis

Manufacturing

3.4   Knee Trajectory Testing

Chapter 4

Parameterization of Human Knee Joints

Chapter 5

Conclusion & Future Work

References

[1] D. L. Benoit, D. K. Ramsey, M. Lamontagne, L. Xu, P. Wretenberg, and P. Renström, "Effect of skin movement artifact on knee kinematics during gait and cutting motions measured in vivo," *Gait & Posture*, vol. 24, no. 2, pp. 152–164, 2006, ISSN: 0966-6362. DOI: `https://doi.org/10.1016/j.gaitpost.2005.04.012`. [Online]. Available: `https://www.sciencedirect.com/science/article/pii/S0966636205001700`.

[2] F. Bertolucci, S. Di Martino, D. Orsucci, E. C. Ienco, G. Siciliano, B. Rossi, M. Mancuso, and C. Chisari, "Robotic gait training improves motor skills and quality of life in hereditary spastic paraplegia," *NeuroRehabilitation*, vol. 36, no. 1, pp. 93–99, 2015.

[3] A. Bjerkefors, M. Carpenter, A. Cresswell, and A. Thorstensson, "Trunk muscle activation in a person with clinically complete thoracic spinal cord injury," *Journal of rehabilitation medicine : official journal of the UEMS European Board of Physical and Rehabilitation Medicine*, vol. 41, pp. 390–2, May 2009. DOI: `10.2340/16501977-0336`.

32

[4] M. Bortole, A. Venkatakrishnan, F. Zhu, J. C. Moreno, G. E. Francisco, J. L. Pons, and J. L. Contreras-Vidal, "The h2 robotic exoskeleton for gait rehabilitation after stroke: Early findings from a clinical study," *Journal of neuroengineering and rehabilitation*, vol. 12, no. 1, pp. 1–14, 2015.

[5] A. Bosch, "Incomplete traumatic quadriplegia. a ten-year review," *JAMA: The Journal of the American Medical Association*, vol. 216, no. 3, pp. 473–478, 1971. DOI: 10.1001/jama.216.3.473.

[6] M. M. B. S. D Wrisley, "Aerobic capacity in early paraplegia: Implications for rehabilitation," *Spinal Cord*, vol. 27, no. 4, pp. 261–268, 1989. DOI: https://doi.org/10.1038/sc.1989.39.

[7] V. Dietz, "Body weight supported gait training: From laboratory to clinical setting," *Brain Research Bulletin*, vol. 76, no. 5, pp. 459–463, 2008, ISSN: 0361-9230. DOI: https://doi.org/10.1016/j.brainresbull.2008.02.034. [Online]. Available: https://www.sciencedirect.com/science/article/pii/S0361923008001111.

[8] Z.-A. Han, J. Y. Choi, and Y. J. Ko, "Dermatological problems following spinal cord injury in korean patients," *The Journal of Spinal Cord Medicine*, vol. 38, no. 1, pp. 63–67, 2013. DOI: 10.1179/2045772313y.0000000154.

[9] L. Harvey, R. Herbert, and J. Crosbie, "Does stretching induce lasting increases in joint rom? a systematic review.," *Physiotherapy research international : the journal for researchers and clinicians in physical therapy*, vol. 7 1, pp. 1–13, 2002.

[10] P. Hill, V. Vedi, A. Williams, H. Iwaki, V. Pinskerova, and M. Freeman, "Tibiofemoral movement 2: The loaded and unloaded living knee studied by mri," *The Journal of Bone and Joint Surgery. British volume*, vol. 82-B, pp. 1196–1198, Nov. 2000. DOI: 10.1302/0301-620X.82B8.0821196.

[11] J. Hwang, Y. Shin, J.-h. Park, Y. J. Cha, and J. (H. You, "Effects of walkbot gait training on kinematics, kinetics, and clinical gait function in paraplegia and quadriplegia," *NeuroRehabilitation*, vol. 42, no. 4, 2018.

[12] F. Ishaque and M. Shamim, "Rehabilitation of paraplegia," *J. Baqai Medical University Health Science*, vol. 11, no. 1, pp. 23–29, Jun. 2008. [Online]. Available: https://applications.emro.who.int/imemrf/Baqai_J_Health_Sci/Baqai_J_Health_Sci_2008_11_1_23_29.pdf.

[13] H. Iwaki, V. Pinskerova, and M. Freeman, "Tibiofemoral movement 1: The shapes and relative movements of the femur and tibia in the unloaded cadaver knee," *The Journal of Bone and Joint Surgery. British volume*, vol. 82-B, pp. 1189–1195, Nov. 2000. DOI: 10.1302/0301-620X.82B8.0821189.

[14] Y. Kimura and S. Hirokawa, "Model analysis of lower limb at ascending from deep knee flexion," 2009.

[15] M. Lafortune, P. Cavanagh, H. Sommer, and A. Kalenak, "Three-dimensional kinematics of the human knee during walking," *Journal of Biomechanics*, vol. 25, no. 4, pp. 347–357, 1992, ISSN: 0021-9290. DOI: https://doi.org/10.1016/0021-9290(92)90254-X. [Online]. Avail-

able: `https://www.sciencedirect.com/science/article/pii/002192909290254X`.

[16] K.-M. Lee and J. Guo, "Kinematic and dynamic analysis of an anatomically based knee joint," *Journal of Biomechanics*, vol. 43, no. 7, pp. 1231–1236, 2010, ISSN: 0021-9290. DOI: `https://doi.org/10.1016/j.jbiomech.2010.02.001`. [Online]. Available: `http://www.sciencedirect.com/science/article/pii/S0021929010000321`.

[17] J. Madorsky and A. Madorsky, "Wheelchair racing: An important modality in acute rehabilitation after paraplegia," *Archives of physical medicine and rehabilitation*, vol. 64, no. 4, pp. 186–187, Apr. 1983, ISSN: 0003-9993. [Online]. Available: `http://europepmc.org/abstract/MED/6838349`.

[18] I. Odéen and E. Knutsson, "Evaluation of the effects of muscle stretch and weight load in patients with spastic paraplegia," *Scandinavian journal of rehabilitation medicine*, vol. 13, no. 4, pp. 117–121, 1981, ISSN: 0036-5505. [Online]. Available: `http://europepmc.org/abstract/MED/7347432`.

[19] *Quadriplegia and paraplegia*. [Online]. Available: `https://www.winchesterhospital.org/health-library/article?id=96908`.

[20] *Spinal cord injury: Flexibility exercises*. [Online]. Available: `https://www.uofmhealth.org/health-library/ug2762`.

[21] V. A. Subra Mani, "Design, development and characterization of a wrap spring clutch/brake mechanism as a knee joint for a hybrid exoskeleton,"

Thesis, Worcester Polytechnic Institute, 100 Institute Road, Worcester MA 01609-2280 USA, May 2020.

[22] Terry J. EllapenHenriette V. HammillMariette SwanepoelGert L. Strydom, "The benefits of hydrotherapy to patients with spinal cord injuries," *African Journal of Disability*, vol. 7, no. 0, 2018. DOI: 10.4102/ajod.v7i0.450.

[23] L. van de Venis, B. P. C. van de Warrenburg, V. Weerdesteyn, B. J. H. van Lith, A. C. H. Geurts, and J. Nonnekes, "Improving gait adaptability in patients with hereditary spastic paraplegia," *Trials*, vol. 22, no. 32, 2021.

Appendix A

Joint Power/Torque/Speed Calculations

Input (Motor) Power	P_{input}	$90 Watts$
Input (Motor) Torque @ Nominal	τ_{input}	$0.560 Nm$
Input (Motor) Speed @ Nominal	ω_{input}	$2510 rpm$
Input (Motor) Stall Torque	τ_{in_stall}	$7.480 Nm$
Gearbox Ration	$\frac{n_1}{n_2}$	$100 : 1$

Table A.1: Motor/Gearbox Specifications

Power Calculation

$$P_{output} = \varepsilon P_{input} = 0.9 * 90W = 81W \tag{A.1}$$

Torque Calculation

$$\tau_{output} = \varepsilon \tau_{input} \frac{n_1}{n_2} = 0.9 * 0.560 Nm * \frac{100}{1} = 50.4 Nm \qquad \text{(A.2)}$$

Speed Calculation

$$\omega_{output} = \omega_{input} \frac{n_2}{n_1} = 2510 rpm * \frac{100}{1} = 2.510 rpm = 15°/sec \qquad \text{(A.3)}$$

Output Power	P_{output}	$81 Watts$
Output Torque @ Nominal	τ_{input}	$50.4 Nm$
Output Speed @ Nominal	ω_{input}	$15°/sec$
Output Stall Torque	τ_{out_stall}	$673.2 Nm$

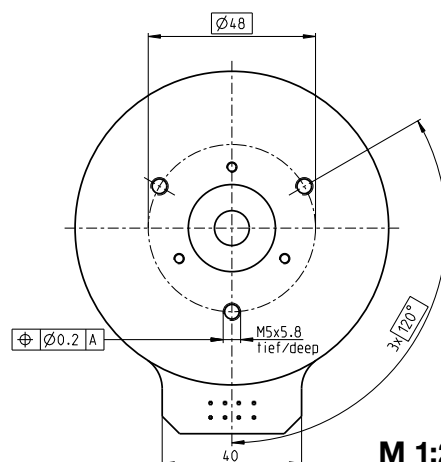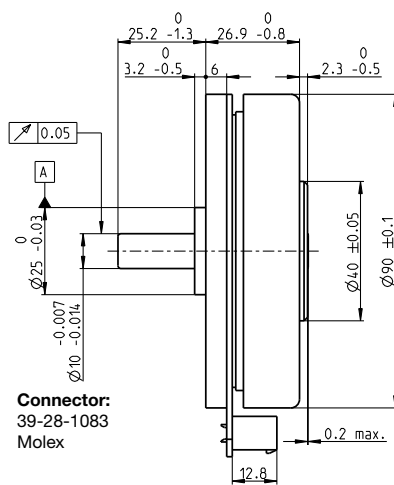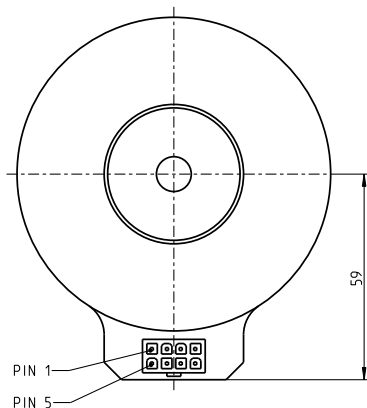Table A.2: Joint Output Specifications

Appendix B

Maxon Motor EC90 Datasheet

Below is the datasheet for the motor chosen for this project: Maxon EC90 part number 429271 (highlighted)

EC 90 flat ∅90 mm, brushless, 90 Watt

Connector:
39-28-1083
Molex

PIN 1
PIN 5

∅48

M 1:2

M5x5.8
tief/deep

■ Stock program
□ Standard program
☐ Special program (on request)

Part Numbers

		with Hall sensors	323772	429271	244879						
Motor Data											
	Values at nominal voltage										
1	Nominal voltage	V	24	36	48						
2	No load speed	rpm	3190	3120	2080						
3	No load current	mA	544	348	135						
4	Nominal speed	rpm	2590	2510	1610						
5	Nominal torque (max. continuous torque)	mNm	444	560	533						
6	Nominal current (max. continuous current)	A	6.06	4.76	2.27						
7	Stall torque	mNm	4940	7480	4570						
8	Stall current	A	70	69	21.1						
9	Max. efficiency	%	84	87	85						
	Characteristics										
10	Terminal resistance phase to phase	Ω	0.343	0.522	2.28						
11	Terminal inductance phase to phase	mH	0.264	0.625	2.5						
12	Torque constant	mNm/A	70.5	109	217						
13	Speed constant	rpm/V	135	88	44						
14	Speed/torque gradient	rpm/mNm	0.659	0.423	0.462						
15	Mechanical time constant	ms	21.1	13.6	14.8						
16	Rotor inertia	gcm²	3060	3060	3060						

Specifications

Thermal data
17 Thermal resistance housing-ambient 1.91 K/W
18 Thermal resistance winding-housing 2.6 K/W
19 Thermal time constant winding 46 s
20 Thermal time constant motor 283 s
21 Ambient temperature -40…+100°C
22 Max. winding temperature +125°C

Mechanical data (preloaded ball bearings)
23 Max. speed 5000 rpm
24 Axial play at axial load < 15 N 0 mm
　　　　　　　　　　　　　　> 15 N 0.14 mm
25 Radial play preloaded
26 Max. axial load (dynamic) 12 N
27 Max. force for press fits (static) 183 N
　　(static, shaft supported) 8000 N
28 Max. radial load, 5 mm from flange 68 N

Other specifications
29 Number of pole pairs 12
30 Number of phases 3
31 Weight of motor 600 g

Values listed in the table are nominal.

Connection
Pin 1　　Hall sensor 1
Pin 2　　Hall sensor 2
Pin 3　　V$_{Hall}$ 4.5…18 VDC
Pin 4　　Motor winding 3
Pin 5　　Hall sensor 3
Pin 6　　GND
Pin 7　　Motor winding 1
Pin 8　　Motor winding 2
Wiring diagram for Hall sensors see p. 43

Cable
Connection cable Universal, L = 500 mm **339380**
Connection cable to EPOS2, L = 500 mm **354045**

Operating Range　　Comments

n [rpm]

90 W

244879
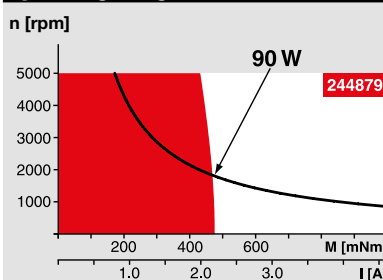
■ **Continuous operation**
In observation of above listed thermal resistance (lines 17 and 18) the maximum permissible winding temperature will be reached during continuous operation at 25°C ambient.
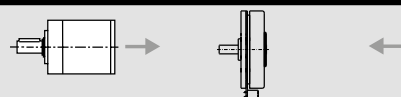= Thermal limit.

□ **Short term operation**
The motor may be briefly overloaded (recurring).

— **Assigned power rating**

maxon Modular System　　

Planetary Gearhead
∅52 mm
4 - 30 Nm
Page 351

Encoder MILE
512 - 6400 CPT,
2 channels
Page 390

Recommended Electronics:
Notes	Page **32**
ESCON Mod. 50/4 EC-S	427
ESCON Mod. 50/5	427
ESCON 50/5	428
ESCON 70/10	428
DEC Module 50/5	430
EPOS2 24/5, 50/5, 70/10	435
EPOS2 P 24/5	438
EPOS4 Module/CB 50/5	442
EPOS4 Module 50/8	443
EPOS4 Comp. 50/8 CAN	443
MAXPOS 50/5	447